

Demonstrating drug treatment efficacies by monitoring superoxide dynamics in human lung cancer cells with time-lapse fluorescence microscopy

Shalaka Konjalwar¹, Busenur Ceyhan¹, Oscar Rivera¹, Parisa Nategh¹, Mehrnoosh Neghabi¹, Mirjana Pavlovic¹, Shailaja Allani¹, and Mahsa Ranji¹

¹Florida Atlantic University

August 21, 2023

Abstract

Metformin hydrochloride, an antihyperglycemic agent, and sulindac, a nonsteroidal anti-inflammatory drug, are FDA-approved drugs known to exert anticancer effects. Previous studies demonstrated sulindac and metformin's anticancer properties through mitochondrial dysfunction and inhibition of mitochondrial electron transport chain (ETC) complex I, as well as key signaling pathways. In this study, various drugs were administered to A549 lung cancer cells, and results revealed that a combination of sulindac and metformin enhanced cell death compared to administration of the drugs separately. To measure superoxide production over time, we employed a time-lapse fluorescence imaging technique using mitochondrial-targeted hydroethidine. Fluorescence microscopy data showed largest increases in superoxide production in the combination treatment of metformin and sulindac. Results showed significant differences between the combined drug treatment and control groups, as well as between the positive control and control groups. This approach can be utilized to quantify anticancer efficacy of drugs, creating possibilities for additional therapeutic options.

RESEARCH ARTICLE

Demonstrating drug treatment efficacies by monitoring superoxide dynamics in human lung cancer cells with time-lapse fluorescence microscopy

Shalaka Konjalwar^{+,1} | Busenur Ceyhan^{+,1} | Oscar Rivera² | Parisa Nategh¹ | Mehrnoosh Neghabi¹ | Mirjana Pavlovic³ | Shailaja Allani² | Mahsa Ranji^{*,1}

1 Department of Electrical Engineering and Computer Science at Florida Atlantic University, Boca Raton, United States of America

2 Center for Molecular Biology and Biotechnology at Florida Atlantic University, Boca Raton, United States of America

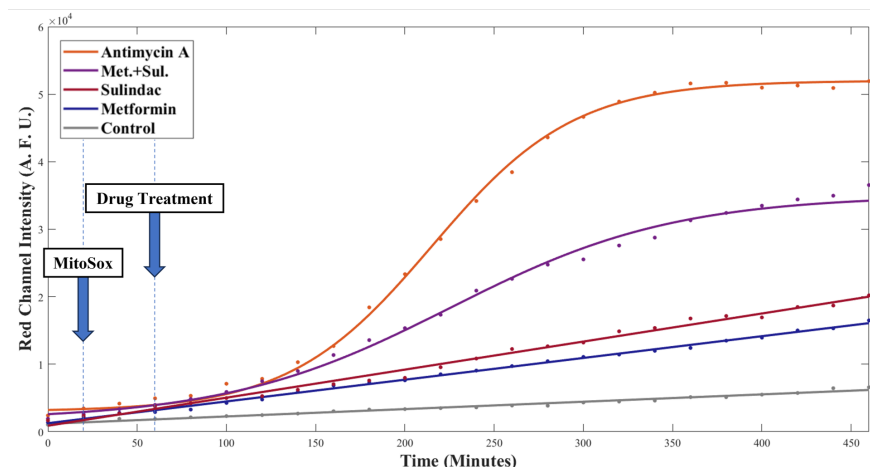
+ Authors should be considered joint first author.

* Correspondence

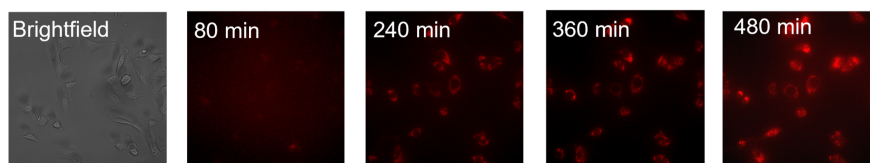
Mahsa Ranji, Department of Electrical Engineering and Computer Science at Florida Atlantic University, Boca Raton, United States of America

Email: mranji@fau.edu

Calibrated intensity profiles in response to drug treatments



Fluorescent images of superoxide production over time in response to combinatorial metformin and sulindac treatment



Metformin hydrochloride, an antihyperglycemic agent, and sulindac, a nonsteroidal anti-inflammatory drug, are FDA-approved drugs known to exert anticancer effects. Previous studies demonstrated sulindac and metformin's anticancer properties through mitochondrial dysfunction and inhibition of mitochondrial electron transport chain (ETC) complex I, as well as key signaling pathways. In this study, various drugs were administered to A549 lung cancer cells, and results revealed that a combination of sulindac and metformin enhanced cell death compared to administration of the drugs separately. To measure superoxide production over time, we employed a time-lapse fluorescence imaging technique using mitochondrial-targeted hydroethidine. Fluorescence microscopy data showed largest increases in superoxide production in the combination treatment of metformin and sulindac. Results showed significant differences between the combined drug treatment and control groups, as well as between the positive control and control groups. This approach can be utilized to quantify anticancer efficacy of drugs, creating possibilities for additional therapeutic options.

KEYWORDS

antimycin A, fluorescence microscopy, metformin, MitoSOX red, oxidative stress, sulindac, superoxide, time-lapse imaging

1 | INTRODUCTION

Reactive oxygen species (ROS) contain an unpaired electron in their outermost shell, making them extremely reactive ions. They play a critical role in the cell, primarily in maintaining homeostasis and facilitating cellular signaling. In mitochondria, ROS are generated through the movement of electrons across the electron transport chain (ETC) during cellular respiration. The ETC consists of complexes I through IV and enzyme ATP synthase in the inner membrane of the mitochondria. As electrons move through the ETC, a portion of these electrons unintentionally leak and are captured by O_2 , resulting in a continuous production

of superoxide anions ($O_2^{\bullet-}$) on a significant scale [1]. However, antioxidant defense mechanisms, such as manganese superoxide dismutase (MnSOD) in the mitochondrial matrix and copper–zinc superoxide dismutase (CuZnSOD) in the intermembrane space and cytosol, typically quickly convert superoxide ($O_2^{\bullet-}$) to hydrogen peroxide (H_2O_2) [2]. While the production of mitochondrial ROS is a natural result of typical cellular metabolic processes, its accumulation in large quantities is often implicated in the progression of various diseases and injuries [3-9].

ROS have a diverse range of effects on cancer cells; ROS increase migration, proliferation, and tumor progression, as well as induce cell senescence and death [10]. Otto Warburg discovered that in the presence of oxygen, cancer cells produce excess lactate, which he deemed “aerobic glycolysis” to explain that cancer cells exhibit a shift towards glycolysis for energy production, rather than oxidative phosphorylation [11, 12]. Though the Warburg effect initially suggested that the respiration process of cancerous cells is damaged, it is widely understood today that their regulation of glycolysis is instead compromised [13, 14]. When ROS production exceeds permissible levels in cancer cells, antioxidant defense mechanism capabilities are depleted, leading to apoptosis (programmed cell death), which highlights the anti-tumorigenic signaling feature of ROS as a promising cancer therapy option [15].

Sulindac is an FDA-approved non-steroidal anti-inflammatory drug (NSAID) that has demonstrated anti-cancer potency [16-20]. Former studies have shown that treating cancer cells with sulindac and subsequently exposing them to oxidizing agents capable of generating ROS, such as hydrogen peroxide, tert-butyl hydroperoxide (TBHP), and dichloroacetate (DCA), leads to apoptosis [21]. Sulindac is also an inhibitor of cyclooxygenases (COX-1 and COX-2), enzymes that convert arachidonic acid to prostaglandins, which are lipid compounds involved in inflammatory responses [22, 23]. However, experiments with lung cancer cells demonstrated that sulindac’s role as a COX inhibitor is unrelated to its function as a cancer-killing drug [23]. Additionally, data has supported sulindac’s protection of normal cells from oxidative damage, another facet of interest when developing cancer treatments [23]. While sulindac’s ability as a cancer therapy option has been proven, there may be other combinations involving the drug that have yet to be fully understood.

Metformin is a longtime FDA-approved drug of the biguanide class used to treat type 2 diabetes (T2D) and has also become of interest in cancer therapy [24]. Metformin’s pleiotropic effects are primarily due to its interactions with the mitochondria, specifically through inhibition of complex I of the ETC, which interferes with oxidative metabolic activity [25, 26]. In 2005, researchers proposed that the administration of metformin may lead to a reduction in instances of cancer in T2D patients [27]. Studies have shown that metformin’s anticancer properties are attributed to its inhibition of mitochondrial ETC complex I and of crucial signaling pathways [28].

MitoSOX Red is a derivative of hydroethidine (HE) that functions as a fluorescent probe designed for the selective detection of superoxide in mitochondria of live cells [29]. MitoSOX Red has a positively charged phosphonium group that specifically targets the cell-permeative HE derivative to the mitochondria, accumulating in the mitochondrial matrix, where its oxidization by $O_2^{\bullet-}$ produces fluorescence proportionate to the concentration of $O_2^{\bullet-}$ [29, 30]. Numerous studies incorporating different cell lines have used MitoSOX Red for selective detection of superoxide anion [31-36].

Sulindac and metformin are both known to have anticancer effects related to the induction of key apoptotic pathways and mitochondrial mechanisms through the inhibition of complexes in the ETC. Therefore, our approach is designed to monitor superoxide dynamics over time in response to each drug as well as the combination of both drugs.

It is hypothesized that oxidative stress, due to oxidative metabolic mitochondrial dysfunction, may play an important role in the anticancer activity of the combination of metformin and sulindac. The aim of this experiment is to measure superoxide levels in lung cancer cells when exposed to metformin, sulindac, and a combined treatment of metformin and sulindac through time-lapse fluorescence imaging, which provides a measurement of dynamic changes in the slopes of superoxide anion production quantitatively over time.

2 | MATERIALS & METHODS

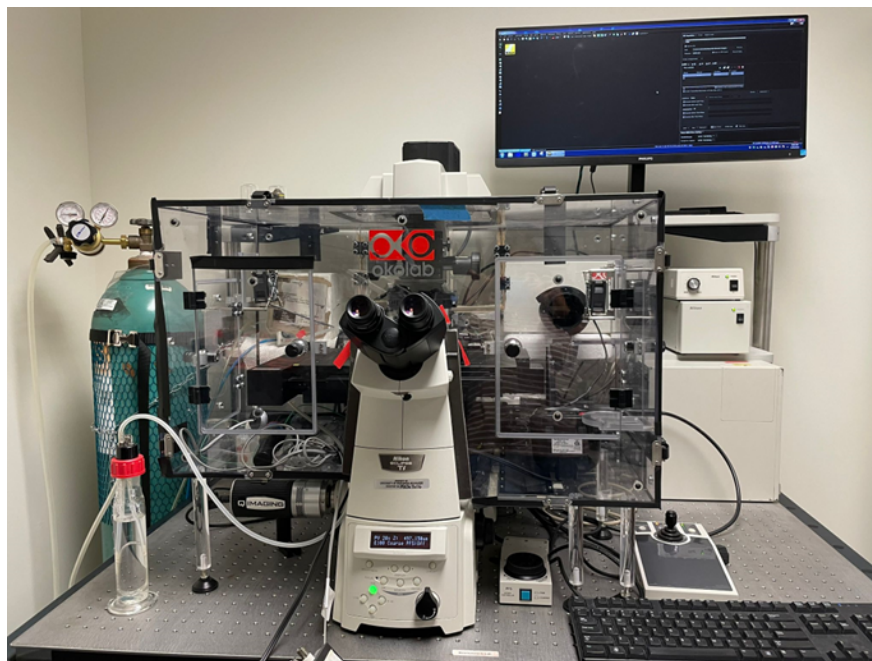
2.1 | Cell Preparation

A549 adenocarcinoma human alveolar basal epithelial lung carcinoma cells were obtained from ATCC (Rockville, MD). The cells were grown in Dulbecco's Modified Eagles Medium (DMEM) (Gibco, Grand Island, NY) and supplemented with 10% FBS (fetal bovine serum) (Gibco, Grand Island, NY), 100 IU/ml penicillin (Gibco, UK), and 100 $\mu\text{g}/\text{ml}$ streptomycin (Gibco, Grand Island, NY), and maintained at 37 and 5% CO_2 in a temperature- and gas-controlled incubator. For repeatability, frozen cell stocks with of the same early passage were prepared.

2.2 | Fluorescence Microscopy

Two days prior to imaging, cells were thawed and seeded to a 24-well plate (50,000 cells/well). Before plating, cell viability was assessed with a Cell Countess II FL Automated Cell Counter (Invitrogen, Carlsbad, CA). A549 cells were cultivated in phenol-free Dulbecco's Modified Eagles Medium (DMEM) (Gibco, Grand Island, NY) and supplemented with 10% FBS (Gibco, Grand Island, NY), 100 IU/ml penicillin (Gibco, Grand Island, NY), and 100 $\mu\text{g}/\text{ml}$ streptomycin (Gibco, Grand Island, NY) and cultured at 37 and 5% CO_2 in a temperature- and gas-controlled incubator. Phenol-free media is used to avoid interference with the red channel dye while imaging [37].

Live cell imaging was performed with a Nikon Ti-E inverted microscope (Nikon Instruments, Melville, NY) customized in the Biophotonics Lab (Florida Atlantic University, Boca Raton, FL) to include a temperature- and gas-controlled incubation chamber (Okolab, Sewickley, PA). An overhead halogen lamp was utilized for brightfield imaging of cells at the beginning of the experiment. Fluorescence excitation was achieved through pairing a mercury arc lamp with a filter cube for the red channel (510 nm) and fluorescent emission was filtered with a filter cube (580 nm) and captured with a Rolera EM-C² CCD camera (Teledyne Photometrics, Tucson, AZ). The imaging protocol begins with a 20-minute baseline imaging session, followed by the addition of 1 μM MitoSOX Red Mitochondrial Superoxide Indicator (Thermo Fisher Scientific, Waltham, MA), where imaging takes place for a duration of 40 minutes. At the 60th minute, cells are subjected to various drug treatments: 25 μM antimycin A (AA, positive control), 250 μM sulindac, 1.6 mM metformin, and a combination of 250 μM sulindac and 1.6 mM metformin. The 8-hour experiment involved capturing images at 20-minute intervals, using 20x magnification and an exposure time of 900 ms. Our experimental protocol is described in detail in previous manuscripts [38-41].



2.3 | Image Processing

Image processing techniques were utilized to retrieve raw intensity profiles from stacks of images for each respective treatment and their duplicates during the 8-hour period of time-lapse fluorescence microscopy. Raw red channel image stacks are processed using ImageJ (National Institutes of Health, Bethesda, MD). First, contrast enhancement is applied to obtain mitochondrial contours. This allows for a ROI (region of interest) to be selected and applied over all 24 images in a stack. For quantification, the selected ROI is used to retrieve mitochondrial fluorescent intensity presented as A.F.U (arbitrary fluorescent units) and background (dark regions) for background subtraction. Intensity profiles are fitted to sigmoidal (Equation 1) and linear (Equation 2) models using MATLAB R2022a (MathWorks Inc., Natick, MA) to visualize trends in drug treatments.

$$y = \frac{1}{1+e^{-x}} \quad (1)$$

$$y = mx + b \quad (2)$$

2.4 | Statistical Analysis

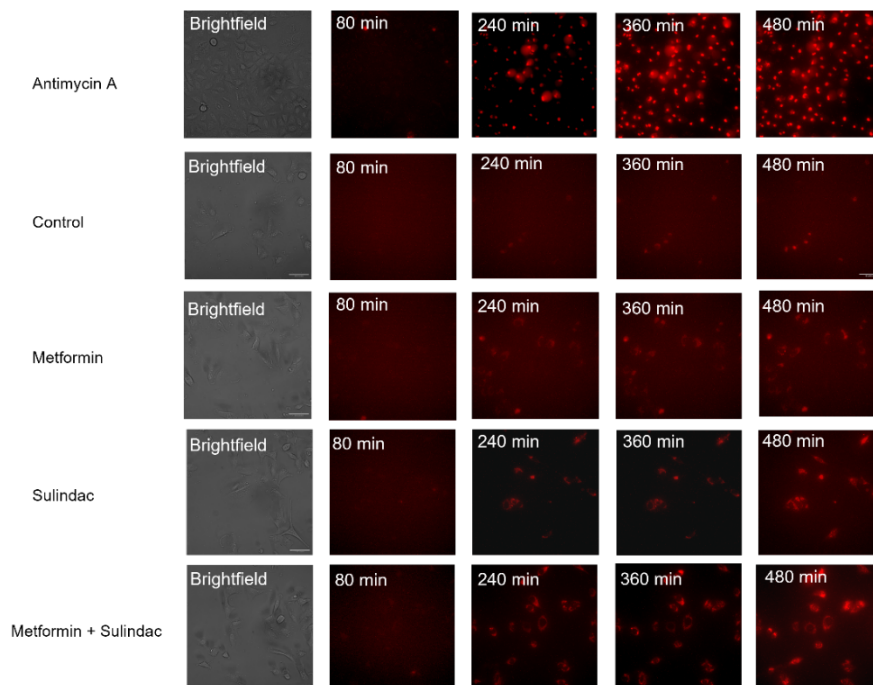
Each condition was repeated 6 times ($n = 6$) with all values represented as the means \pm SD. A one-way ANOVA test with p-value set to $p < 0.05$ was used to determine the statistical significance of each drug treatment and demonstrate the function of differences in treatment conditions as a variable. Relative percent changes were calculated with respect to control considered as zero and signify the production of superoxide for each treatment condition.

2.4 | Cell Viability Assay

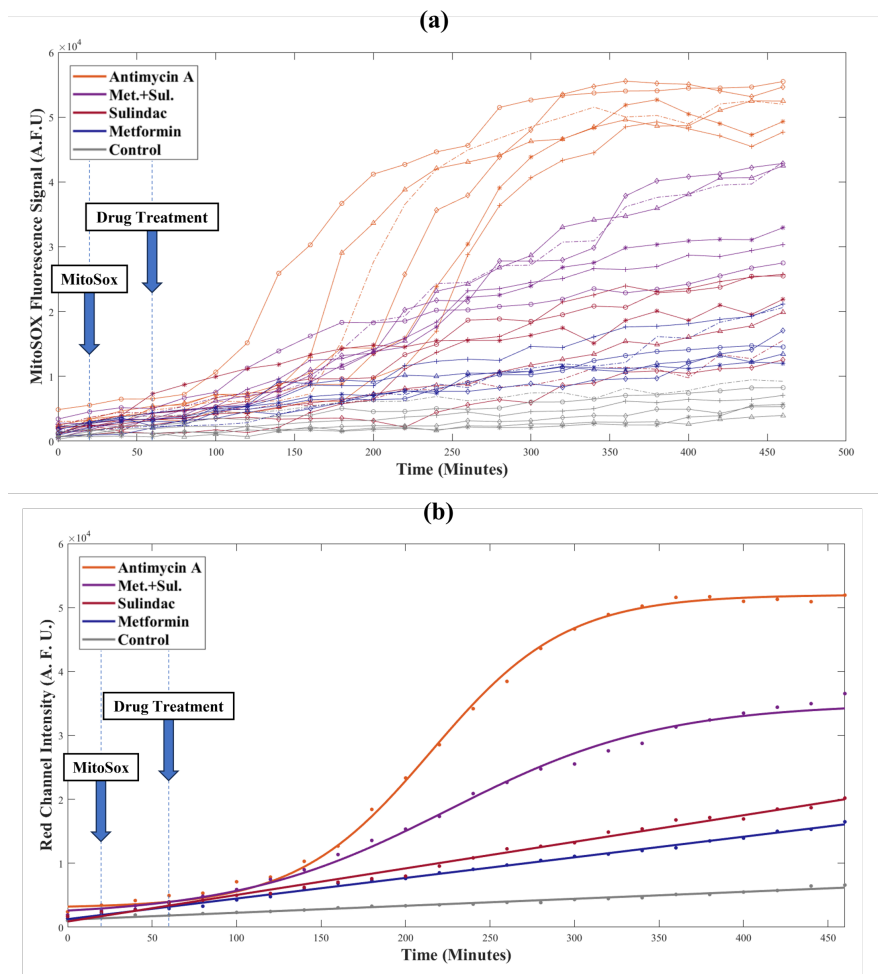
A549 cells were plated at 5×10^3 cells per well in a 96-well plate with 100 μ L of the cell suspension for 24 hours at 37°C and 5% CO₂ in an incubator. The media was then discarded under aseptic conditions before being replaced with media containing 250 μ M of sulindac and varying concentrations of metformin, 400 μ M, 800 μ M, 1.2 mM, 1.6 mM, and 2.0 mM. Cells were incubated for 48 hours in a 37°C and 5% CO₂ incubator. Cell viability was obtained using a CellTiter 96 Aqueous One Cell Proliferation Assay (Promega, Madison, WI) in accordance with the manufacturer's instructions. This assay used a tetrazolium salt compound that is reduced to a water-soluble formazan dye through dehydrogenase enzymes in metabolically active cells [21, 42]. The formazan dye is quantified by measuring its absorbance at 490 nm with a colorimetric microtiter plate reader (SpectraMax Plus 384, Molecular Devices).

3 | RESULTS

The signal from MitoSOX red in A549 cells demonstrated the production of O₂^{*-} by mitochondria under conditions of increased oxidative stress. Figure 1 depicts brightfield and red fluorescent images of A549 cells under the various drug treatment conditions, as well as positive control (AA) and control conditions. The first row is the positive control (AA) group, followed by the control group, and rows three through five are the drug treatment conditions, metformin, sulindac, and combination of metformin and sulindac, respectively. The first column of images contains brightfield images of each treatment group, taken prior to the addition of the fluorescent probe or any drug treatment. The second column of images are taken at 80 minutes, which is 20 minutes after each drug treatment was administered. The third and fourth columns include images taken at 240 minutes and 360 minutes respectively, and visualize increased superoxide anion production as time progresses, over a period of 120 minutes between the two columns. The last column captures intensity after 480 minutes, which is the end point of the experiment. These images demonstrate varying increases in intensities depending on condition. Heightened red fluorescence intensity over time explains increased superoxide production after exposure to treatment conditions.

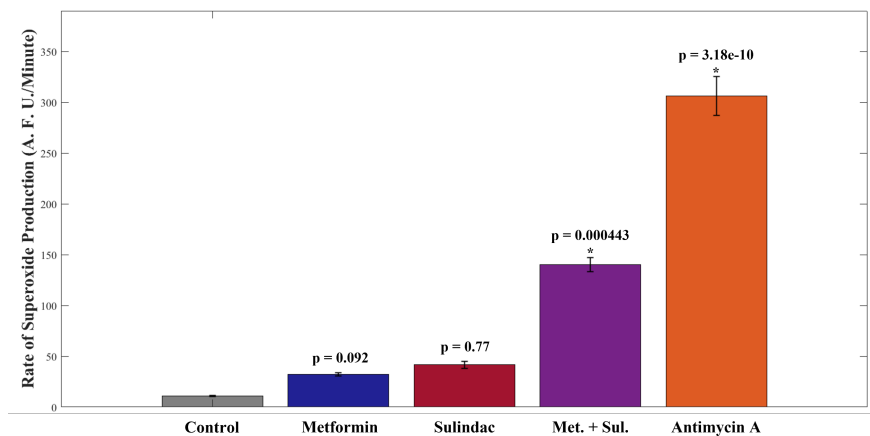


Raw red channel MitoSOX fluorescence signal was plotted over time for each of the five groups using a selected ROI (see Materials & Methods). For consistency and reproducibility, six fields of view (FOVs) were imaged for cells in each treatment group, as well as the positive control and control groups. Figure 3a depicts raw fluorescence intensity for each group ($n = 6$), indicating the time points where MitoSOX Red indicator and drug treatments were added. After administering treatment, an increase in intensity was observed in all groups, implying a surge in the superoxide anion production rate. Additionally, as time increased, treatment groups showed a plateau or gradual increase in slope, validating the chosen duration of 8 hours.

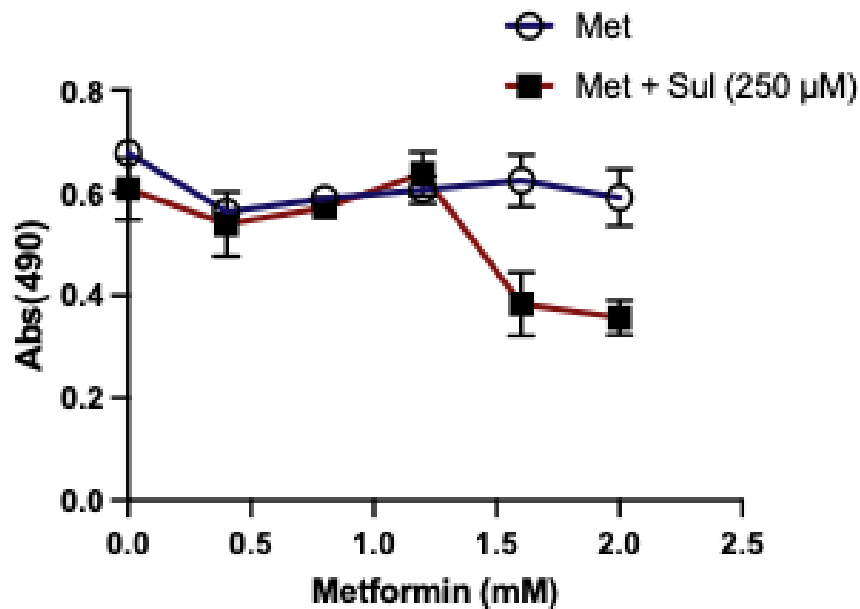


To quantify the rate of superoxide anion production over time in response to the different treatment conditions, sigmoidal and linear equations were fitted to the data (See Materials & Methods). Figure 3b consists of the data fitted to the sigmoidal equation for AA and combination treatment, and linear equation for control, metformin, and sulindac treatments. The nonlinear fitting used for AA and the combination of metformin and sulindac demonstrates a greater increase in the $O_2^{\cdot -}$ production rate in the aforementioned groups in comparison to the remaining groups. This can be further justified by Table 1, where slopes of AA and the combination of metformin and sulindac are notably greater than the linear slopes. Table 2 depicts the percent change between the slopes of the control group and the treatment groups, including AA. The percent change between the control and positive control group is the greatest (75.93%), followed by the difference between the control and combination of metformin and sulindac groups (33.22%), control group and sulindac (7.88%), and lastly control group and metformin (5.48%). The highest difference was expected, as AA is the positive control, though the greater difference in percent change between control and combination group, compared to control and the treatments alone indicates the role of the drug combination in superoxide production increases over time.

The slopes of red channel fluorescence intensity for each group are compared to one another statistically in Figure 4 and showed significant changes in the positive control and combined treatment compared to the control group. In these treatment cases, there was a large difference in the rate of superoxide production over time with respect to the control group, reflecting the effects of the drugs on the mitochondria and its processes.



Cell viability is quantified in Figure 5 and corresponds with the fluorescent intensity data obtained above. Here, different concentrations of metformin (400 μ M, 800 μ M, 1.2 mM, 1.6 mM, and 2.0 mM) were added to A549 cells either in the presence of 250 μ M sulindac or not. When no metformin, 400 μ M metformin, 800 μ M metformin, and 1.2 mM metformin are combined with 250 μ M sulindac, absorbance values remained in the range of \sim 0.5 to \sim 0.7 nm. However, once 250 μ M of sulindac was added to 1.6 mM of metformin, absorbance dropped from \sim 0.6 nm to less than 0.4 nm. This indicated the potency of the combination of 250 μ M and 1.6 mM metformin, as a drastic reduction in cell viability, which corresponds to measured absorbance, was observed. 2.0 mM metformin and 250 μ M sulindac demonstrated analogous outcomes. However, it is advisable to avoid using a drug combination with concentrations that are higher than necessary. The combination of 1.6 mM metformin and 250 μ M sulindac was also used in time-lapse fluorescence imaging, indicating that fluorescence information can be used to validate cell viability data.



4 | DISCUSSION

This study quantifies chemotherapeutic efficacy of drugs metformin, sulindac, and their combination in terms of superoxide production using time-lapse fluorescence microscopy. Superoxide levels were quantified

over an 8-hour period for each treatment through time-lapse fluorescence microscopy. The various drug treatments exhibited distinct trends in the generation of superoxide, as depicted in Figure 2. We report i) the combination of sulindac and metformin mediated robust superoxide generation out of all treatment conditions and ii) individual treatments of metformin and sulindac do not generate an effective response when compared to the combination treatment using the same dosages. These findings suggest the co-treatment to cancer cells could increase apoptosis in the presence of an oxidative agent, functioning as a more effective cancer treatment option.

Previous experiments examined the combination of pre-treatment with sulindac before the addition of another agent and concluded that mitochondrial dysfunction played a role in anticancer mechanisms [21, 23]. This present study is an expansion of this work, as it investigates the onset of cellular effects while the drug combination is administered together, validating cell viability data. Additionally, this study demonstrates in further detail the mechanism of action for superoxide formation and its potential role in cancer cell death.

Cancer research using chemotherapeutic agents indicates evidence of heavily fostered apoptosis of tumor cells by these agents [43-45]. Specifically, research has focused on agents that elevate superoxide levels in cancer tissue, utilizing superoxide to induce apoptotic pathways [46]. Superoxide form key agents of mitochondrial dysfunction often associated with apoptosis-inducing cancer drugs [45]. This coincides with the results from this research where highest superoxide elevation was observed with the combination drug treatment (Figure 4).

The inhibition of complex I by metformin causes superoxide accumulation in the mitochondrial matrix, promoting a collapse of cellular homeostasis and apoptosis [47, 48]. Previous experiments have suggested that administering metformin increased superoxide production, decreased mitochondrial membrane potential, activated caspase family enzymes, which are closely related to apoptosis, increased apoptosis-promoting BAX (BCL-2 associated X protein) levels, and decreased anti-apoptotic BCL-2 (B-cell lymphoma-2) and MCL-1 (Myeloid leukemia 1) protein levels [47, 49-51]. Sulindac-induced apoptosis heavily relies on superoxide generation [23, 45]. The oxidative stress induced by superoxide phosphorylates p38 MAPK (p38 mitogen-activated protein kinase) [52], a protein prominently involved in apoptotic pathways and p53 a tumor suppressor gene [53]. The Bcl-protein family controls proapoptotic responses by the inhibition of BAX and BAK (Bcl-2 homologous antagonist killer) [54, 55]. Cancer cells have been found to evade apoptosis predominantly by inhibiting BAX and BAK proteins [56]. The oligomerization of BAX and BAK at the mitochondrial outer membrane (MOM) opens pores mediating the release of cytochrome c (cyt c) from the mitochondria [56]. Cyt c activates caspases that cleave all cellular components of the cell. Accordingly, administering metformin and sulindac together brings forth significant superoxide accumulation in the mitochondria supporting a chemotherapeutic mechanism for activation of the apoptotic events.

We have demonstrated a combination of two FDA approved drugs with anti-cancer activity can more intensely induce superoxide production in cancer cells than when treated alone. This approach is advantageous because it reduces dosage requirements as well as the development of drug resistance often seen in monotherapies. When drugs with different mechanisms of action are combined, each drug can be used at its optimal dose, limiting adverse side effects. A two-drug treatment can reduce cytotoxicity to peripheral non-tumor cells [57] and provide a more efficacious treatment.

5 | CONCLUSION

Time-lapse microscopy was used to monitor ROS generation in lung cancer cells treated with a combinatorial treatment, metformin and sulindac. Results from this study report significant superoxide accumulation due to the combined effect of metformin and sulindac on A549 lung cancer cells. However, superoxide production for individual metformin and sulindac treatments showed only modest increases. The combinatorial treatment has shown a notable anticancer effect, specifically targeting the metabolic dysfunction caused by excess superoxide, which ultimately may lead to increased cell death in lung cancer cells. This study demonstrates elevated superoxide levels in the dual drug combination, which can be used in chemotherapeutic treatments. We aim to expand on our prior protocol and investigation to quantitatively measure and compare $O_2^{\bullet-}$

production across different cancer treatment conditions [39]. Our ongoing cancer therapy regime examines the influence of extremely low frequency electromagnetic field radiation combined with proapoptotic agents.

ACKNOWLEDGEMENTS

This work was funded by National Institutes of Health (EY031533).

CONFLICT OF INTEREST

The authors declare no conflict of interest.

DATA AVAILABILITY STATEMENT

The data that support the findings of this study are available from the corresponding author upon reasonable request.

REFERENCES

- [1] H. P. Indo *et al.* , "A mitochondrial superoxide theory for oxidative stress diseases and aging," *Journal of Clinical Biochemistry and Nutrition*, vol. 56, no. 1, pp. 1-7, 2015.
- [2] D. F. Stowe and A. K. S. Camara, "Mitochondrial Reactive Oxygen Species Production in Excitable Cells: Modulators of Mitochondrial and Cell Function," *Antioxidants & Redox Signaling*, vol. 11, no. 6, pp. 1373-1414, 2009.
- [3] T. Finkel, "Oxygen radicals and signaling," *Current Opinion in Cell Biology*, vol. 10, no. 2, pp. 248-253, 1998.
- [4] D. G. Harrison and Y. Ohara, "Physiological Consequences of Increased Vascular Oxidant Stresses in Hypercholesterolemia and Atherosclerosis – Implications for Impaired Vasomotion," *American Journal of Cardiology*, Article vol. 75, no. 6, pp. B75-B81, Feb 1995.
- [5] M. Sundaresan, Z.-X. Yu, V. J. Ferrans, K. Irani, and T. Finkel, "Requirement for Generation of H₂O₂ for Platelet-Derived Growth Factor Signal Transduction," *Science*, vol. 270, no. 5234, pp. 296-299, 1995.
- [6] R. M. Touyz, "Reactive oxygen species and angiotensin II signaling in vascular cells: implications in cardiovascular disease," *Brazilian Journal of Medical and Biological Research*, vol. 37, no. 8, pp. 1263-1273, 2004.
- [7] H.-L. Hsieh and C.-M. Yang, "Role of Redox Signaling in Neuroinflammation and Neurodegenerative Diseases," *BioMed Research International*, vol. 2013, pp. 1-18, 2013.
- [8] N. S. Chandel, E. Maltepe, E. Goldwasser, C. E. Mathieu, M. C. Simon, and P. T. Schumacker, "Mitochondrial reactive oxygen species trigger hypoxia-induced transcription," *Proceedings of the National Academy of Sciences*, vol. 95, no. 20, pp. 11715-11720, 1998.
- [9] A. Tosatto *et al.* , "The mitochondrial calcium uniporter regulates breast cancer progression via HIF-1 α ," *EMBO Molecular Medicine*, vol. 8, no. 5, pp. 569-585, 2016.
- [10] P. Storz, "Reactive oxygen species in tumor progression," *FBL*, vol. 10, no. 2, pp. 1881-1896, 2005-05-01 2005.
- [11] O. Warburg, F. Wind, and E. Negelein, "The Metabolism of Tumors in the Body," *J Gen Physiol*, vol. 8, no. 6, pp. 519-30, Mar 7 1927.
- [12] O. Warburg, "On the Origin of Cancer Cells," *Science*, vol. 123, no. 3191, pp. 309-314, 1956.
- [13] W. H. Koppenol, P. L. Bounds, and C. V. Dang, "Otto Warburg's contributions to current concepts of cancer metabolism," *Nature Reviews Cancer*, vol. 11, no. 5, pp. 325-337, 2011/05/01 2011.
- [14] L. Yu, X. Chen, X. Sun, L. Wang, and S. Chen, "The Glycolytic Switch in Tumors: How Many Players Are Involved?," *J Cancer*, vol. 8, no. 17, pp. 3430-3440, 2017.

- [15] S. Arfin *et al.* , "Oxidative Stress in Cancer Cell Metabolism," *Antioxidants*, vol. 10, no. 5, p. 642, 2021.
- [16] G. A. Piazza *et al.* , "NSAIDs: Old Drugs Reveal New Anticancer Targets," *Pharmaceuticals*, vol. 3, no. 5, pp. 1652-1667, 2010.
- [17] C. V. Rao *et al.* , "Chemoprevention of Colon Carcinogenesis by Sulindac, a Nonsteroidal Anti-inflammatory Agent," *Cancer Research*, vol. 55, no. 7, pp. 1464-1472, 1995.
- [18] M. Richter, M. Weiss, I. Weinberger, G. Furstenberger, and B. Marian, "Growth inhibition and induction of apoptosis in colorectal tumor cells by cyclooxygenase inhibitors," *Carcinogenesis*, vol. 22, no. 1, pp. 17-25, 2001.
- [19] M. M. Taketo, "Cyclooxygenase-2 Inhibitors in Tumorigenesis (Part II)," *JNCI: Journal of the National Cancer Institute*, vol. 90, no. 21, pp. 1609-1620, 1998.
- [20] M. M. Taketo, "Cyclooxygenase-2 Inhibitors in Tumorigenesis (Part I)," *JNCI: Journal of the National Cancer Institute*, vol. 90, no. 20, pp. 1529-1536, 1998.
- [21] K. S. Ayyanathan K, Dawson-Scully K, Weissbach H, "Combination of Sulindac and Dichloroacetate Kills Cancer Cells via Oxidative Damage.," *PLOS ONE*, vol. 7, no. 7, 2012.
- [22] S. H. Choi, S. Aid, and F. Bosetti, "The distinct roles of cyclooxygenase-1 and -2 in neuroinflammation: implications for translational research," *Trends Pharmacol Sci*, vol. 30, no. 4, pp. 174-81, Apr 2009.
- [23] M. Marchetti, Resnick, L., Gamliel, E., Kesaraju, S., Weissbach, H., Binninger, D., "Sulindac Enhances the Killing of Cancer Cells Exposed to Oxidative Stress," *PLOS ONE*, vol. 4, no. 6, 2009.
- [24] M. Foretz, Guigas, B., Bertrand, L., Pollak, M., Viollet, B., "Metformin: From Mechanisms of Action to Therapies," *Cell Metabolism*, vol. 20, no. 6, pp. 953-966, 2014.
- [25] M. El-Mir, Nogueira, V., Fontaine, E., Avéret, N., Rigoulet, M., Leverve, X., "Dimethylbiguanide Inhibits Cell Respiration via an Indirect Effect Targeted on the Respiratory Chain Complex I*," *Journal of Biological Chemistry*, vol. 275, no. 1, pp. 223-228, 2000.
- [26] M. R. Owen, E. Doran, and A. P. Halestrap, "Evidence that metformin exerts its anti-diabetic effects through inhibition of complex 1 of the mitochondrial respiratory chain," *Biochemical Journal*, vol. 348, no. 3, pp. 607-614, 2000.
- [27] J. M. Evans, L. A. Donnelly, A. M. Emslie-Smith, D. R. Alessi, and A. D. Morris, "Metformin and reduced risk of cancer in diabetic patients," *Bmj*, vol. 330, no. 7503, pp. 1304-5, Jun 4 2005.
- [28] J. Dong *et al.* , "Metformin mediated microRNA-7 upregulation inhibits growth, migration, and invasion of non-small cell lung cancer A549 cells," *Anticancer Drugs*, vol. 31, no. 4, pp. 345-352, Apr 2020.
- [29] P. Mukhopadhyay, M. Rajesh, G. Haskó, B. J. Hawkins, M. Madesh, and P. Pacher, "Simultaneous detection of apoptosis and mitochondrial superoxide production in live cells by flow cytometry and confocal microscopy," *Nat Protoc*, vol. 2, no. 9, pp. 2295-301, 2007.
- [30] K. M. Robinson *et al.* , "Selective fluorescent imaging of superoxide in vivo using ethidium-based probes," *Proc Natl Acad Sci U S A*, vol. 103, no. 41, pp. 15038-43, Oct 10 2006.
- [31] M. E. Kauffman *et al.* , "MitoSOX-Based Flow Cytometry for Detecting Mitochondrial ROS," *React Oxyg Species (Apex)*, vol. 2, no. 5, pp. 361-370, 2016.
- [32] N. Kundu *et al.* , "Sucralose promotes accumulation of reactive oxygen species (ROS) and adipogenesis in mesenchymal stromal cells," *Stem Cell Research & Therapy*, vol. 11, no. 1, p. 250, 2020/06/26 2020.
- [33] P. Mukhopadhyay, M. Rajesh, K. Yoshihiro, G. Haskó, and P. Pacher, "Simple quantitative detection of mitochondrial superoxide production in live cells," *Biochemical and Biophysical Research Communications*,

vol. 358, no. 1, pp. 203-208, 2007/06/22/ 2007.

[34] K. M. Robinson, M. S. Janes, and J. S. Beckman, "The selective detection of mitochondrial superoxide by live cell imaging," *Nature Protocols*, vol. 3, no. 6, pp. 941-947, 2008/06/01 2008.

[35] H. Rottenberg and S. Wu, "Quantitative assay by flow cytometry of the mitochondrial membrane potential in intact cells," *Biochimica et Biophysica Acta (BBA) - Molecular Cell Research*, vol. 1404, no. 3, pp. 393-404, 1998/09/16/ 1998.

[36] J.-T. Yang, Z.-L. Li, J.-Y. Wu, F.-J. Lu, and C.-H. Chen, "An Oxidative Stress Mechanism of Shikonin in Human Glioma Cells," *PLOS ONE*, vol. 9, no. 4, p. e94180, 2014.

[37] A. Ettinger and T. Wittmann, "Fluorescence live cell imaging," *Methods Cell Biol*, vol. 123, pp. 77-94, 2014.

[38] Z. Ghanian, G. G. Konduri, S. H. Audi, A. K. S. Camara, and M. Ranji, "Quantitative optical measurement of mitochondrial superoxide dynamics in pulmonary artery endothelial cells," *J Innov Opt Health Sci*, vol. 11, no. 1, 2018.

[39] Z. Ghanian, S. Mehrvar, N. Jamali, N. Sheibani, and M. Ranji, "Time-lapse microscopy of oxidative stress demonstrates metabolic sensitivity of retinal pericytes under high glucose condition," *Journal of Biophotonics*, vol. 11, no. 9, p. e201700289, 2018.

[40] Z. Ghanian, R. Sepehr, A. Eis, G. Kondouri, and M. Ranji, *Optical Studies of Oxidative Stress in Pulmonary Artery Endothelial Cells* (SPIE BiOS). SPIE, 2015.

[41] S. Mehrvar, Z. Ghanian, G. Kondouri, A. Camara, and M. Ranji, *Time-lapse microscopy of lung endothelial cells under hypoxia* (SPIE BiOS). SPIE, 2017.

[42] A. H. Cory, T. C. Owen, J. A. Barltrop, and J. G. Cory, "Use of an Aqueous Soluble Tetrazolium/Formazan Assay for Cell Growth Assays in Culture," *Cancer Communications*, vol. 3, no. 7, pp. 207-212, // 1991.

[43] T. A. Chan, P. J. Morin, B. Vogelstein, and K. W. Kinzler, "Mechanisms underlying nonsteroidal antiinflammatory drug-mediated apoptosis," *Proc Natl Acad Sci U S A*, vol. 95, no. 2, pp. 681-6, Jan 20 1998.

[44] H. J. Thompson *et al.* , "Sulfone metabolite of sulindac inhibits mammary carcinogenesis," *Cancer Res*, vol. 57, no. 2, pp. 267-71, Jan 15 1997.

[45] S. K. Seo *et al.* , "Sulindac-derived reactive oxygen species induce apoptosis of human multiple myeloma cells via p38 mitogen activated protein kinase-induced mitochondrial dysfunction," *Apoptosis*, vol. 12, no. 1, pp. 195-209, Jan 2007.

[46] M. Redza-Dutordoir and D. A. Averill-Bates, "Activation of apoptosis signalling pathways by reactive oxygen species," *Biochim Biophys Acta*, vol. 1863, no. 12, pp. 2977-2992, Dec 2016.

[47] Z. Y. Gao *et al.* , "Metformin induces apoptosis via a mitochondria-mediated pathway in human breast cancer cells in vitro," *Exp Ther Med*, vol. 11, no. 5, pp. 1700-1706, 2016/05/01 2016.

[48] H. U. Simon, A. Haj-Yehia, and F. Levi-Schaffer, "Role of reactive oxygen species (ROS) in apoptosis induction," *Apoptosis*, vol. 5, no. 5, pp. 415-418, 2000/11/01 2000.

[49] M. D. Aldea *et al.* , "Metformin plus sorafenib highly impacts temozolomide resistant glioblastoma stem-like cells," *J buon*, vol. 19, no. 2, pp. 502-11, Apr-Jun 2014.

[50] A. B. Haugrud, Y. Zhuang, J. D. Coppock, and W. K. Miskimins, "Dichloroacetate enhances apoptotic cell death via oxidative damage and attenuates lactate production in metformin-treated breast cancer cells," *Breast Cancer Res Treat*, vol. 147, no. 3, pp. 539-50, Oct 2014.

- [51] E. H. Kim, M. S. Kim, C. K. Cho, W. G. Jung, Y. K. Jeong, and J. H. Jeong, "Low and high linear energy transfer radiation sensitization of HCC cells by metformin," *J Radiat Res*, vol. 55, no. 3, pp. 432-42, May 2014.
- [52] A. Kulisz, N. Chen, N. S. Chandel, Z. Shao, and P. T. Schumacker, "Mitochondrial ROS initiate phosphorylation of p38 MAP kinase during hypoxia in cardiomyocytes," *Am J Physiol Lung Cell Mol Physiol*, vol. 282, no. 6, pp. L1324-9, Jun 2002.
- [53] B. Liu, Y. Chen, and D. K. St Clair, "ROS and p53: a versatile partnership," *Free Radic Biol Med*, vol. 44, no. 8, pp. 1529-35, Apr 15 2008.
- [54] J. L. Perfettini *et al.* , "Essential role of p53 phosphorylation by p38 MAPK in apoptosis induction by the HIV-1 envelope," *J Exp Med*, vol. 201, no. 2, pp. 279-89, Jan 17 2005.
- [55] B. J. Kim, S. W. Ryu, and B. J. Song, "JNK- and p38 kinase-mediated phosphorylation of Bax leads to its activation and mitochondrial translocation and to apoptosis of human hepatoma HepG2 cells," *J Biol Chem*, vol. 281, no. 30, pp. 21256-21265, Jul 28 2006.
- [56] J. Lopez and S. W. Tait, "Mitochondrial apoptosis: killing cancer using the enemy within," *Br J Cancer*, vol. 112, no. 6, pp. 957-62, Mar 17 2015.
- [57] H. Maeda and M. Khatami, "Analyses of repeated failures in cancer therapy for solid tumors: poor tumor-selective drug delivery, low therapeutic efficacy and unsustainable costs," *Clin Transl Med*, vol. 7, no. 1, p. 11, Mar 1 2018.